


Collective Excitations of a Strongly Correlated Nonequilibrium Photon Fluid across the Insulator-Superfluid Phase Transition

Fabio Caleffi^{1,*}, Massimo Capone^{1,2}, and Iacopo Carusotto³

¹*International School for Advanced Studies (SISSA), Via Bonomea 265, I-34136 Trieste, Italy*

²*CNR-IOM Democritos, Via Bonomea 265, I-34136 Trieste, Italy*

³*INO-CNR BEC Center and Dipartimento di Fisica, Università di Trento, Via Sommarive 14, I-38123 Povo, Italy*

 (Received 26 November 2022; revised 15 July 2023; accepted 26 September 2023; published 9 November 2023)

We develop a Gutzwiller theory for the nonequilibrium steady states of a strongly interacting photon fluid driven by a non-Markovian incoherent pump. In particular, we explore the collective modes of the system across the out-of-equilibrium insulator-superfluid transition of the system, characterizing the diffusive Goldstone mode in the superfluid phase and the excitation of particles and holes in the insulating one. Observable features in the pump-and-probe optical response of the system are highlighted. Our predictions are experimentally accessible to state-of-the-art circuit-QED devices and open the way for the study of novel driven-dissipative many-body scenarios with no counterparts at equilibrium.

DOI: [10.1103/PhysRevLett.131.193604](https://doi.org/10.1103/PhysRevLett.131.193604)

Introduction.—Quantum fluids of light are rapidly growing as a new branch of many-body physics [1,2]. Right after the observation of Bose-Einstein condensation [3], superfluidity [4] and hydrodynamic generation of topological excitations [5,6] in weakly interacting polariton fluids in semiconductor microcavities, exciting advances in circuit-QED engineering [7–9] are preparing the ground for the realization of strongly interacting fluids [10–13] in bosonic lattice models [14–17]. Thanks to the strong effective photon-photon interactions, these systems are promising candidates to explore Bose-Hubbard physics [18] and the insulator-superfluid quantum phase transition [19–22] in a novel out-of-equilibrium context.

In this regard, pioneering theoretical investigations have explored the rich variety of nonequilibrium steady states (NESS) under coherent pumping protocols or Markovian incoherent ones [23–26], also in comparison with the corresponding equilibrium systems [27]. Generalizing to scenarios with non-Markovian incoherent pumping [28–30] provide us with a whole new direction [31], as non-Markovian features proved crucial for the experimental creation of genuine insulating states in strongly interacting regimes [32].

These experimental advances call for theoretical approaches able to investigate the nature of the observed steady states. This is a challenging task bridging the quantum optics, condensed matter, and many-body communities and requires us to establish a common language and an interdisciplinary perspective across these fields. Among the open issues, we mention the collective properties and dynamical correlations of out-of-equilibrium insulators and strongly interacting superfluids. Even though various techniques are available to describe driven-dissipative systems, such as mean-field theories [1], variational

methods [29,33–36], matrix-product states [30,37–41], and clustering techniques [42], major hurdles still persist in the extension of these methods to the dynamics of large, high-dimensional, and strongly interacting non-Markovian systems [29–31].

In this Letter, we make use of the Gutzwiller ansatz—a simple yet powerful description of Mott physics in generic condensed matter systems [43–46]—and we extend it to the nonequilibrium context of strongly interacting photons in a cavity array under a non-Markovian and incoherent pump. The properties of the collective excitation spectrum across the insulating and superfluid phases are characterized, and novel features stemming from the nonequilibrium condition are highlighted. Our predictions represent a first step towards the understanding of quantum fluctuations in strongly correlated out-of-equilibrium many-body systems. Observable fingerprints are identified in the response of the system to additional weak probes, which is directly accessible to experiments based on modern circuit-QED technology.

Model and mean-field theory.—We consider a translationally invariant d -dimensional array of coupled optical cavities modeled by a Bose-Hubbard (BH) Hamiltonian,

$$\hat{H}_{\text{BH}} = \sum_{\mathbf{r}} (\omega_c \hat{a}_{\mathbf{r}}^\dagger \hat{a}_{\mathbf{r}} + U \hat{a}_{\mathbf{r}}^\dagger \hat{a}_{\mathbf{r}}^\dagger \hat{a}_{\mathbf{r}} \hat{a}_{\mathbf{r}}) - J \sum_{\langle \mathbf{r}, \mathbf{s} \rangle} \hat{a}_{\mathbf{r}}^\dagger \hat{a}_{\mathbf{s}}, \quad (1)$$

where $\hat{a}_{\mathbf{r}} (\hat{a}_{\mathbf{r}}^\dagger)$ is the annihilation (creation) operator associated with the cavity mode at site \mathbf{r} , J is the hopping energy, ω_c is the bare cavity frequency, and U is the photon-photon interaction energy stemming from the optical nonlinearity of the cavity medium [1,2]. Systems of this kind are currently used for the preparation and

manipulation of a variety of target quantum states of the microwave field in state-of-the-art circuit-QED platforms, e.g., by embedding superconducting qubit elements, such as transmons, in arrays of coupled coplanar waveguide resonators and by suitably designing both the conservative and dissipative terms of the dynamics [12,13,32,47,48].

The driven-dissipative dynamics of the BH array involves photon losses at a rate Γ_l and the coupling of each cavity mode to incoherently pumped two-level emitters (TLEs). The dynamics of the TLEs is governed by the Hamiltonian

$$\hat{H}_{\text{em}} = \omega_{\text{at}} \sum_{\mathbf{r}} \hat{\sigma}_{\mathbf{r}}^+ \hat{\sigma}_{\mathbf{r}}^- + \Omega \sum_{\mathbf{r}} (\hat{a}_{\mathbf{r}}^\dagger \hat{\sigma}_{\mathbf{r}}^- + \text{H.c.}), \quad (2)$$

where $\hat{\sigma}_{\mathbf{r}}^\pm$ is the rising (lowering) operator in the pseudospin space of each TLE and the Rabi frequency Ω quantifies their coupling to the cavities. The TLEs are pumped via some Markovian mechanism at a rate Γ_p and decay at a rate γ . In order to achieve an efficient photon injection into the cavity modes, we assume $\Gamma_p \gg \gamma$, which results in population-inverted TLEs. Most notably, this provides a straightforward realization of a non-Markovian driving protocol for the cavity modes, with an energy-dependent gain peaked at the TLE frequency ω_{at} with linewidth approximately equal to Γ_p [29]. This form of pumping has been predicted to give a high-fidelity emulation of the BH model [30].

The evolution of the system is described by the Lindblad equation for the full density matrix $\hat{\rho}$,

$$\begin{aligned} \partial_t \hat{\rho} = & -i[\hat{H}_{\text{BH}} + \hat{H}_{\text{em}}, \hat{\rho}] \\ & + \frac{1}{2} \sum_{\mathbf{r}} (\Gamma_l \mathcal{D}[\hat{a}_{\mathbf{r}}; \hat{\rho}] + \gamma \mathcal{D}[\hat{\sigma}_{\mathbf{r}}^-; \hat{\rho}] + \Gamma_p \mathcal{D}[\hat{\sigma}_{\mathbf{r}}^+; \hat{\rho}]), \end{aligned} \quad (3)$$

where $\mathcal{D}[\hat{O}; \hat{\rho}] = 2\hat{O}\hat{\rho}\hat{O}^\dagger - \{\hat{O}^\dagger\hat{O}, \hat{\rho}\}$. For later convenience, we introduce the parameter $G \equiv \Omega^2/(\Gamma_p\Gamma_l)$, which defines the effective strength of the photon injection process [49]. A pictorial sketch of the model is provided in the top panel of Fig. 1.

In this Letter, we study the system within a mean-field description based on a Gutzwiller ansatz [26,27,59]. This consists in a site-factorized ansatz for the density matrix,

$$\hat{\rho} = \otimes_{\mathbf{r}} \sum_{n,m} \sum_{\sigma,\sigma'} c_{n,m,\sigma,\sigma'}(\mathbf{r}) |n, \sigma\rangle_{\mathbf{r}} \langle m, \sigma'|_{\mathbf{r}}, \quad (4)$$

where $|n, \sigma\rangle_{\mathbf{r}}$ is the local state of the cavity at \mathbf{r} with n cavity photons and TLE pseudospin σ . In this way, the Lindblad equation turns into a set of nonlinear dynamical equations for the (vectorized) density matrix elements $i\partial_t \vec{c}(\mathbf{r}) = \hat{L}[\vec{c}(\mathbf{r})] \cdot \vec{c}(\mathbf{r})$. In order to get the NESS, we solve these equations by numerical propagation until convergence to the steady-state $\hat{\rho}_0 = \hat{\rho}(t \rightarrow \infty)$. As we are considering a translationally invariant system, this

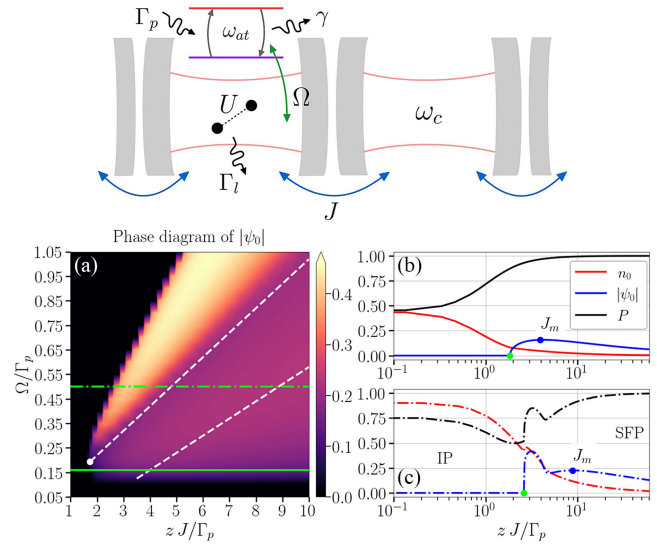


FIG. 1. Top panel: sketch of the driven-dissipative system under consideration. (a) Mean-field phase diagram of the NESS for $\Gamma_l/\Gamma_p = 50/\Gamma_p = 5 \times 10^{-2}$. The solid (dashed) green line corresponds to the horizontal cut at $\Omega/\Gamma_p = 1.6 \times 10^{-1}$ (5×10^{-1}) shown in panel (b) [panel (c)]. The white point marks the tip of the SFP lobe, while the white dashed lines enclose the region of hole superfluidity. (b) Mean-field average density n_0 [red], order parameter $|\psi_0|$ [blue] and purity P [black] across the IP-SFP transition at constant $\Omega/\Gamma_p = 1.6 \times 10^{-1}$ for the same parameters of panel (a). The green and blue dots highlight the critical point J_c and the hopping scale J_m , respectively. (c) The equivalent of panel (b) for a stronger pumping $\Omega/\Gamma_p = 5 \times 10^{-1}$.

corresponds to a \mathbf{r} -independent form $\vec{c}(\mathbf{r}) = \vec{c}_0$ of the Gutzwiller ansatz [49]. Note how the Gutzwiller ansatz (4) provides a nonperturbative description of the on-site dynamics (2), which is able to capture the pump and loss processes up to the strong pumping regime $G \gtrsim 1$, as well as the strong photon-photon interactions. While the Gutzwiller approximation provides an accurate description of both the insulating and superfluid phases [60], deviations are likely to appear in the vicinity of the critical point, where nonlocal correlations are typically substantial. A study of this physics is postponed to future work based on our quantum Gutzwiller ansatz [60].

In this Letter, we restrict ourselves to the hard-core limit of our model ($U/J \rightarrow \infty$), intended as an archetypal scenario of the strong photon nonlinearity regimes that are currently attainable in circuit-QED experiments [10,12,13,32]. Moreover, we choose to set the TLE frequency to $\omega_{\text{at}} = \omega_c - zJ$ (with $z = 2d$), in order to favor photon injection into the states at the bottom of the cavity band. This guarantees that complex spatial fragmentation and/or finite- \mathbf{k} condensation effects do not take place and one can focus on condensation into the lowest-energy $\mathbf{k} = 0$ state as in equilibrium systems [61]. In this regime, the main properties of the NESS can be summarized as follows [49].

Insulator-superfluid nonequilibrium phase transition.—At fixed Ω and below a critical hopping J_c , the NESS is found to be in an insulating phase (IP) with vanishing order parameter $\psi_0 = \text{Tr}(\hat{\rho}_0 \hat{a})$. In particular, for a large enough pumping $G \gg 1$ and $J \lesssim J_c$, the average photon density $n_0 = \text{Tr}(\hat{\rho}_0 \hat{n})$ reaches a value close to 1 with suppressed number fluctuations [Fig. 1(c)], as in an essentially pure Mott insulating state [29,32]. Increasing the cavity bandwidth zJ , i.e., the kinetic energy, replenishment of lost photons occurs less efficiently, which leads to a substantial decrease in the density, alongside some entropy generation. At $J = J_c$, the NESS undergoes a second-order phase transition [62] to a superfluid phase (SFP), developing a finite order parameter displaying limit cycles $\psi_0 = |\psi_0| e^{-i\omega_0 t}$ and scaling as $|\psi_0| \sim \sqrt{J - J_c}$ [63]. In the $\Omega - J$ projection of the phase diagram [Fig. 1(a)], the SFP occupies a lobe-shaped region.

We stress that this IP-SFP transition is not due to a competition between delocalization and local interactions as usual in the equilibrium BH model, but rather stems from a *filling effect* determined by the competition between the emission bandwidth Γ_p and the characteristic kinetic energy J of particles and holes. As such, it can also occur in the hard-core limit under consideration here: for a large Γ_p/J , all states in the cavity band are filled and the system behaves as an insulator, while for smaller Γ_p/J the photon occupation is concentrated in the lower part of the band, which leads to the onset of coherence and superfluidity.

In the SFP, the average total density n_0 is an overall decreasing function of J , which acts similarly to a chemical potential for the system. Indeed, the oscillation or lasing frequency of the coherent field shows only a little deviation from its mean-field value at equilibrium, i.e., $\omega_0 \approx zJ(2n_0 - 1) + \omega_c$ [49], meaning that the energy is lowered at large J by depleting photons. On the other hand, the condensate density $\rho_c = |\psi_0|^2$ is generally a nonmonotonic function of J and its behavior crucially depends on the value of Ω . In the moderate pumping regime $G \sim 1$, located below the tip of the SFP lobe [Fig. 1(b)], ρ_c shows a maximum for $J = J_m$, after which it saturates n_0 to give an extremely pure and dilute condensate. This behavior can be understood as follows. For $J < J_m$, local losses Γ_l play a key role in favoring quantum coherence: since they make the condensate density to increase while reducing n_0 , the NESS can be classified as a *hole superfluid* [64,65]. For $J > J_m$, the large bandwidth zJ overcomes the effect of all dissipative effects, so that cavity photons form a dilute *particle superfluid*, whose purity increases with J [66]. Interestingly, in the strong pumping regime $G \gtrsim 1$ [Fig. 1(c)], a second maximum of ρ_c develops for $J_c < J < J_m$, corresponding to a particle superfluid nearing the equilibrium hard-core state [49].

Collective excitations.—Inspired by well-known linearization methods at equilibrium [67,68], we make use of the approach introduced in [26] and consider small, spatially

dependent oscillations around the NESS configuration as described by the space- and time-dependent Gutzwiller ansatz

$$\vec{c}(\mathbf{r}, t) = \vec{c}_0 + \vec{u}_{\mathbf{k}} e^{i(\mathbf{k}\cdot\mathbf{r} - \omega_{\mathbf{k}} t)} + \vec{v}_{\mathbf{k}}^* e^{-i(\mathbf{k}\cdot\mathbf{r} - \omega_{\mathbf{k}}^* t)}. \quad (5)$$

Here, $\vec{u}_{\mathbf{k}}(\vec{v}_{\mathbf{k}})$ weighs a particle (hole) excitation with energy $\omega_{\mathbf{k}}(-\omega_{\mathbf{k}}^*)$ and the ansatz (5) is seen from the rotating frame of the coherent field [49]. Linearizing its evolution with respect to the oscillation amplitudes, one obtains the Bogoliubov–de Gennes equations

$$\omega_{\mathbf{k}} \begin{pmatrix} \vec{u}_{\mathbf{k}} \\ \vec{v}_{\mathbf{k}} \end{pmatrix} = \hat{\mathcal{L}}_{\mathbf{k}} \begin{pmatrix} \vec{u}_{\mathbf{k}} \\ \vec{v}_{\mathbf{k}} \end{pmatrix}, \quad (6)$$

where the superoperator $\hat{\mathcal{L}}_{\mathbf{k}}$ is block diagonal because of the Hermiticity relation $\vec{v}_{\mathbf{k}} = (\vec{u}_{\mathbf{k}})^T$ [49]. As a main result of this Letter, the eigenvalue equation (6) provides the energy spectra $\omega_{\alpha, \mathbf{k}}$ of the collective many-body excitations of the NESS as well as the strength of the system response to different perturbation channels [49].

Insulating phase.—The low-energy part [49] of the excitation spectrum in the IP phase [Figs. 2(a)–2(a’)] consists of two dispersive branches $\omega_{\pm}(\mathbf{k}) = \pm \varepsilon_{\text{ph}}(\mathbf{k}) - i\Gamma_{\text{ph}}(\mathbf{k})$

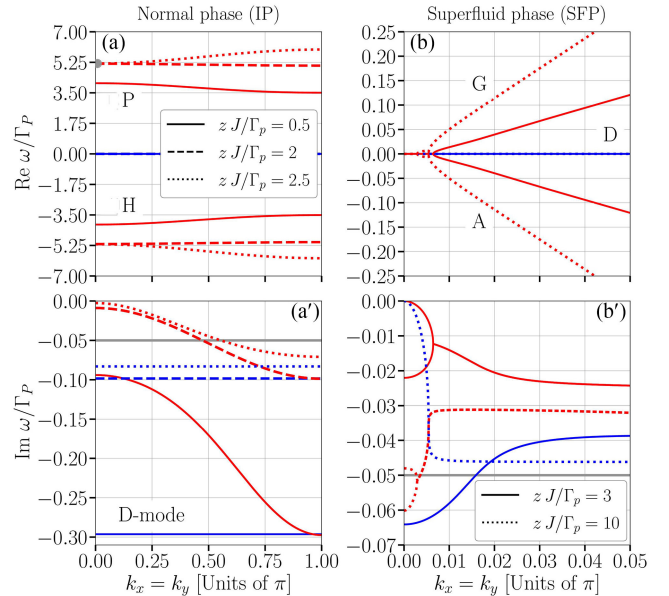


FIG. 2. (a)–(a’) Excitation spectrum of the IP for $\Omega/\Gamma_p = 5 \times 10^{-1}$ [see Fig. 1(c)] and increasing zJ/Γ_p . The gray dot in panel (a) pinpoints the critical lasing frequency ω_* . (b)–(b’) Excitation spectrum of the SFP for $\Omega/\Gamma_p = 3 \times 10^{-1}$ and two values of zJ/Γ_p below/above the antiadiabatic crossover at $J = J_m$ (solid-dashed). The letters G, A, and D indicate the (standard) Goldstone, amplitude and D-mode branches. Here, the excitation energy is calculated in the rotating frame of the lasing frequency ω_0 . In panels (a)–(b’), the gray solid line specifies the cavity loss rate Γ_l/Γ_p . All panels refer to a $d = 2$ array.

(red lines) and a purely dissipative local mode $\omega_D = -i\Gamma_D$ (blue lines), to which we refer as the *D mode*. The former bands correspond to distinct *particle* (*P*) and *hole* (*H*) excitations in the photon fluid, while the latter only involves fluctuations of the TLEs excited state population. Deep in the IP phase (solid lines), the *P* (*H*) damping $\Gamma_{\text{ph}}(\mathbf{k})$ has a gapped, quadratic dispersion which extends up to the energy scale of the effective pumping rate $\Gamma_{\text{em}} \simeq 4\Omega^2/\Gamma_p$ [49]. This indicates that delocalized *P* and *H* excitations at small $|\mathbf{k}|$ have a longer lifetime. As the hopping reaches the lasing threshold J_c (dotted lines), the imaginary part Γ_D of the *D*-mode frequency approaches the bare loss rate Γ_l [gray solid line in Fig. 2(a)], while the one $\Gamma_{\text{ph}}(\mathbf{0})$ of the longest-lived mode corresponding to the Liouvillian gap vanishes proportionally to the distance from the critical point $J_c - J$ [62] as expected from quantum field theory [69]: this substantiates the physical picture of long-lived *P* and *H* modes as precursors of the nonequilibrium transition to the SFP.

Tuning the hopping has a dramatic effect also on the real part of the *P* (*H*) excitation energy shown in Fig. 2(a), which is well fitted by $\varepsilon_{\text{ph}}(\mathbf{k}) \approx J(\mathbf{k})(1 - 2n_0) + \omega_c$ [where $J(\mathbf{k})$ is the free-particle dispersion on the lattice] and is characterized by a density-dependent bandwidth. In detail, at small J where $n_0 > 1/2$, $\varepsilon_{\text{ph}}(\mathbf{k})$ has an *inverted* profile with minimal gap at $\mathbf{k} = \boldsymbol{\pi}$, while a more standard quadratic dispersion is found at larger J when $n_0 < 1/2$. In between the two regimes, an intermediate value of J is found for which $n_0 = 1/2$, and the *P* (*H*) band is completely flat (dashed lines). Eventually, $\varepsilon_{\text{ph}}(\mathbf{0})$ nears the lasing frequency $\omega_* = \omega_0(J = J_c)$ (gray dot) at the IP-SFP transition point, which therefore can be regarded as an authentic finite-frequency criticality [63,70].

Superfluid phase.—As the onset of the SFP corresponds to a spontaneous breaking of U(1) symmetry, the *P* mode is replaced by a Goldstone branch whose complex frequency tends to zero in the long-wavelength limit, $\omega_G(\mathbf{k} \rightarrow 0) \rightarrow 0$ [70,71]. Physically, this mode can be understood as a slow rotation of the condensate phase across the cavity array. Let us analyze the main features of different SFP regimes in more detail, starting from the region $J \lesssim J_m$.

For this case, a typical example of the excitation spectrum is given by the solid lines in Figs. 2(b)–2(b'). Here, we recover in a novel strongly correlated regime the usual behavior of out-of-equilibrium condensates with a diffusive and nonpropagating $\text{Im}\omega_G(\mathbf{k}) \sim -\mathbf{k}^2$ behavior of the low- \mathbf{k} Goldstone mode (red line) [72–75] and a gapped *amplitude* mode with a finite imaginary part $\text{Im}\omega_A(\mathbf{k})$ in the low- \mathbf{k} limit [72,75]. The nontrivial dispersion of the *D* mode $\omega_D(\mathbf{k}) \sim -i\Gamma_l$ in our configuration and its relationship with the Goldstone branch are pivotal to grasping the physics of the deep SFP.

In this $J \lesssim J_m$ regime, there is a clear scale separation between the imaginary part of the Goldstone energy $\Gamma_G(\mathbf{k})$ and the *D* mode $\omega_D(\mathbf{k})$, which, however, gets reduced for increasing J . The above situation changes dramatically at

the boundary between particle and hole superfluidity $J = J_m$: here, the timescales of pumping and loss processes are comparable so the dissipative dynamics of the TLEs can no longer be adiabatically separated from that of the photons in the BH lattice. This translates into a stable cross hybridization of the *D*-mode $\omega_D(\mathbf{k})$ with the Goldstone branch $\Gamma_G(\mathbf{k})$ at small momenta, which anyway leaves the real part of the energy spectrum unaltered [dashed lines in Figs. 2(b)–2(b')].

Dynamical response to a weak probe.—Further light on the collective modes can be obtained from the linear response functions of the NESS to an additional weak coherent probe beam that is able to inject or remove particles from the system [76],

$$\hat{H}_p = \sum_{\mathbf{r}} (\eta_{\mathbf{k},\omega} e^{i(\mathbf{k}\cdot\mathbf{r}-\omega t)} \hat{a}_{\mathbf{r}}^\dagger + \text{H.c.}). \quad (7)$$

In particular, we focus on the corresponding retarded Green's function, whose Fourier-space form $G_R(\mathbf{k}, \omega)$ directly provides the *transmission* $T(\mathbf{k}, \omega) = -i\Gamma_l G_R(\mathbf{k}, \omega)$ and the *reflection* $R(\mathbf{k}, \omega) = 1 + T(\mathbf{k}, \omega)$ amplitudes for a weak probe beam of wave vector \mathbf{k} and frequency ω [1,77,78]. For these experimentally accessible quantities, our theory provides a semianalytical result $G_R(\mathbf{k}, \omega) = \sum_{\alpha} Z_{\alpha,\mathbf{k}} / (\omega - \omega_{\alpha,\mathbf{k}})$ displaying poles at the collective mode frequencies [49].

In the deep IP, we find that the transmittivity $|T(\mathbf{k}, \omega)|^2$ [49] displays a peak at the *P* excitation pole but remains well below unity. In contrast, the reflectivity [Fig. 3(a)] exhibits amplification as $|R(\mathbf{k}, \omega)|^2 > 1$. This result is tightly linked with the intrinsic out-of-equilibrium nature of the IP. While for the transmittivity we simply have $|T(\mathbf{k}, \omega)| \propto |G_R(\mathbf{k}, \omega)|$, the reflectivity reads

$$|R(\mathbf{k}, \omega)|^2 = [1 - \pi\Gamma_l^2 A(\mathbf{k}, \omega)]^2 + \Gamma_l^4 |\text{Re}G_R(\mathbf{k}, \omega)|^2 \quad (8)$$

and can be greater than 1 when the density of states (DOS) $A(\mathbf{k}, \omega) \propto -\text{Im}G_R(\mathbf{k}, \omega)$ is *negative*, see Fig. 3(a). The DOS negativity, already observed in the presence of Markovian dissipation [63,79,80], is a signature of the pump-induced population inversion taking place in the deep IP and is conventionally associated with optical gain [81–83] analogous to the one of a laser device driven below threshold. Still, it is not yet able to support a macroscopic coherence. Thus, we can draw a Janus-faced portrait of the IP state: while it lacks long-range coherence and behaves as an insulator from the viewpoint of many-body excitations, its dynamical response features a broadband amplification distributed along the whole energy dispersion of the *P* mode.

Upon increasing J , the *P* branch $\varepsilon_{\text{ph}}(\mathbf{k})$ is shifted to larger energies and gradually crosses the critical lasing frequency ω_* . Interestingly, ω_* acts here as an effective chemical potential, as the DOS smoothly acquires a

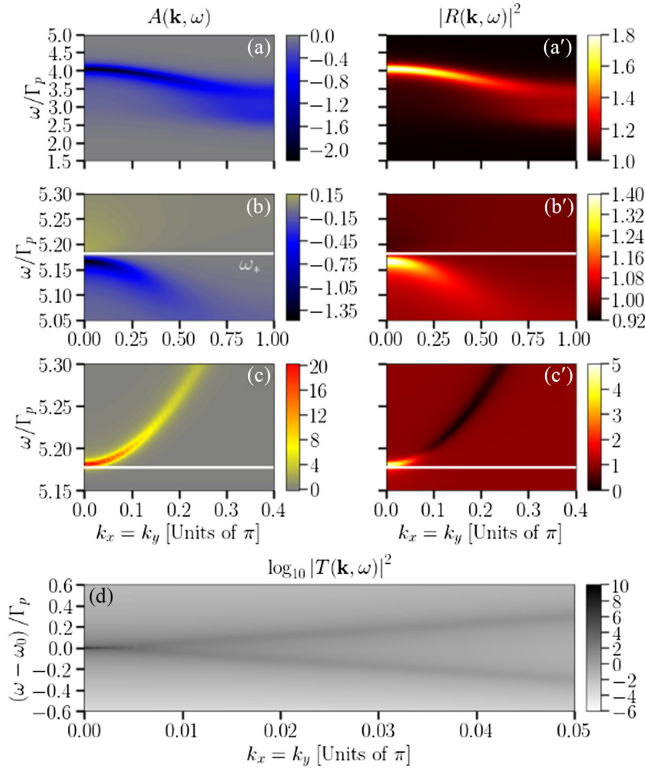


FIG. 3. (a)–(c) DOS in the IP for the same parameters of Figs. 2(a)–2(a) and increasing values of zJ/Γ_p (from top to bottom) towards the critical point. (a)–(c) The related reflectivity spectrum. The white horizontal lines indicate the effective chemical potential ω_* . (d) Transmittivity in the SFP corresponding to the excitation spectra in Figs. 2(b)–2(b) for $zJ/\Gamma_p = 10$ (antiadiabatic regime).

positive sign for $\omega > \omega_*$. This spectral redistribution strongly reflects on the IP response, especially when the P band becomes flat [Figs. 3(b)–3(b)]. In particular, whereas the transmittivity concentrates around the condensation point ($\mathbf{k} = \mathbf{0}, \omega_*$), the reflectivity has a Fano-like shape around ω_* : namely, $|R(\mathbf{k}, \omega)|^2$ is above (below) 1 for $\omega < \omega_*$ ($> \omega_*$), because of the sign flip of the DOS. Eventually, in proximity of the critical point [Figs. 3(c)–3(c)], the DOS becomes mostly positive and bounded by ω_* from below, while the divergence of $\text{Re}G_R(\mathbf{k}, \omega)$ around ω_* [63] marks the onset of condensation. This is visible as a dramatic increase of the low- \mathbf{k} response when approaching the transition, similarly to the diverging amplification displayed by a laser device as the pump strength reaches the threshold. Still, as a key difference from a standard laser, coherence appears at our IP-SFP transition as the photon modes get depleted below unit filling for increasing J/Γ_p .

On the SFP side, the behavior of our strongly interacting system differs from other out-of-equilibrium superfluids [84] in that the transmittivity and reflectivity are able to clearly resolve both the Goldstone and ghost

branches [Fig. 3(d)]. In analogy with strongly interacting BH superfluids at equilibrium [65], this can be explained in terms of the strong nonlinearity and the emergent particle-hole symmetry of the low- \mathbf{k} excitations [49].

Conclusions.—In this Letter, we have developed a Gutzwiller approach to the collective excitations of a driven-dissipative fluid of light in the regime of strong photon-photon interactions, focusing on the nonequilibrium insulator-superfluid transition of the system. In particular, our results highlight experimentally accessible signatures of the surprising peculiarities of the nonequilibrium insulating state, shown to enable light amplification in a pump-and-probe configuration, and of the rich interplay between coherence and dissipation underlying the diffusive nature of the Goldstone mode. Thanks to its flexibility, our theory paves the way to a more general understanding of the exotic quantum phases that emerge in lattice systems driven out of equilibrium and can find experimental realization in the next generation of circuit-QED experiments.

Stimulating discussions with M. Schirò, A. Biella, M. Seclì, and M. Stefanini are warmly acknowledged. F.C. and M.C. acknowledge financial support from the Italian MIUR under the PRIN 2017 “CEnTraL” project (Prot. 20172H2SC4 005) and PRIN 2020 (Prot. 2020JLZ52N 002). I.C. acknowledges financial support from the European Union H2020-FETFLAG-2018-2020 project “PhoQuS” (n.820392), from the Provincia Autonoma di Trento, from the Q@TN Initiative, and from the PNRR MUR project PE0000023-NQSTI.

*bafioc11@gmail.com

- [1] I. Carusotto and C. Ciuti, *Rev. Mod. Phys.* **85**, 299 (2013).
- [2] M. J. Hartmann, *J. Opt.* **18**, 104005 (2016).
- [3] R. Balili, V. Hartwell, D. Snoko, L. Pfeiffer, and K. West, *Science* **316**, 1007 (2007).
- [4] A. Amo, J. Lefrère, S. Pigeon, C. Adrados, C. Ciuti, I. Carusotto, R. Houdré, E. Giacobino, and A. Bramati, *Nat. Phys.* **5**, 805 (2009).
- [5] G. Nardin, G. Grosso, Y. Léger, B. Piętko, F. Morier-Genoud, and B. Deveaud-Plédran, *Nat. Phys.* **7**, 635 (2011).
- [6] D. Sanvitto, S. Pigeon, A. Amo, D. Ballarini, M. D. Giorgi, I. Carusotto, R. Hivet, F. Pisanello, V.G. Sala, P.S.S. Guimaraes, R. Houdré, E. Giacobino, C. Ciuti, A. Bramati, and G. Gigli, *Nat. Photonics* **5**, 610 (2011).
- [7] A. Imamoglu, H. Schmidt, G. Woods, and M. Deutsch, *Phys. Rev. Lett.* **79**, 1467 (1997).
- [8] J. Cho, D. G. Angelakis, and S. Bose, *Phys. Rev. Lett.* **101**, 246809 (2008).
- [9] J. M. Fink, M. Göppl, M. Baur, R. Bianchetti, P. J. Leek, A. Blais, and A. Wallraff, *Nature (London)* **454**, 315 (2008).
- [10] A. A. Houck, H. E. Türeci, and J. Koch, *Nat. Phys.* **8**, 292 (2012).
- [11] R. Barends, J. Kelly, A. Megrant, D. Sank, E. Jeffrey, Y. Chen, Y. Yin, B. Chiaro, J. Mutus, C. Neill, P. O’Malley,

- P. Roushan, J. Wenner, T. C. White, A. N. Cleland, and J. M. Martinis, *Phys. Rev. Lett.* **111**, 080502 (2013).
- [12] P. Roushan *et al.*, *Science* **358**, 1175 (2017).
- [13] I. Carusotto, A. A. Houck, A. J. Kollár, P. Roushan, D. I. Schuster, and J. Simon, *Nat. Phys.* **16**, 268 (2020).
- [14] M. J. Hartmann, F. G. S. L. Brandão, and M. B. Plenio, *Nat. Phys.* **2**, 849 (2006).
- [15] A. D. Greentree, C. Tahan, J. H. Cole, and L. C. L. Hollenberg, *Nat. Phys.* **2**, 856 (2006).
- [16] J.-B. You, W. L. Yang, Z.-Y. Xu, A. H. Chan, and C. H. Oh, *Phys. Rev. B* **90**, 195112 (2014).
- [17] C. Noh and D. G. Angelakis, *Rep. Prog. Phys.* **80**, 016401 (2016).
- [18] M. P. A. Fisher, P. B. Weichman, G. Grinstein, and D. S. Fisher, *Phys. Rev. B* **40**, 546 (1989).
- [19] D. G. Angelakis, M. F. Santos, and S. Bose, *Phys. Rev. A* **76**, 031805(R) (2007).
- [20] A. Tomadin, V. Giovannetti, R. Fazio, D. Gerace, I. Carusotto, H. E. Türeci, and A. Imamoglu, *Phys. Rev. A* **81**, 061801(R) (2010).
- [21] C.-W. Wu, M. Gao, Z.-J. Deng, H.-Y. Dai, P.-X. Chen, and C.-Z. Li, *Phys. Rev. A* **84**, 043827 (2011).
- [22] J.-B. You, W.-L. Yang, G. Chen, Z.-Y. Xu, L. Wu, C.-E. Png, and M. Feng, *Opt. Lett.* **44**, 2081 (2019).
- [23] D. Rossini and R. Fazio, *Phys. Rev. Lett.* **99**, 186401 (2007).
- [24] I. Carusotto, D. Gerace, H. E. Türeci, S. De Liberato, C. Ciuti, and A. Imamoglu, *Phys. Rev. Lett.* **103**, 033601 (2009).
- [25] F. Nissen, S. Schmidt, M. Biondi, G. Blatter, H. E. Türeci, and J. Keeling, *Phys. Rev. Lett.* **108**, 233603 (2012).
- [26] A. Le Boité, G. Orso, and C. Ciuti, *Phys. Rev. Lett.* **110**, 233601 (2013).
- [27] A. Le Boité, G. Orso, and C. Ciuti, *Phys. Rev. A* **90**, 063821 (2014).
- [28] E. Kapit, M. Hafezi, and S. H. Simon, *Phys. Rev. X* **4**, 031039 (2014).
- [29] A. Biella, F. Storme, J. Lebreuilly, D. Rossini, R. Fazio, I. Carusotto, and C. Ciuti, *Phys. Rev. A* **96**, 023839 (2017).
- [30] J. Lebreuilly, A. Biella, F. Storme, D. Rossini, R. Fazio, C. Ciuti, and I. Carusotto, *Phys. Rev. A* **96**, 033828 (2017).
- [31] K. Donatella, A. Biella, A. Le Boité, and C. Ciuti, *Phys. Rev. Res.* **2**, 043232 (2020).
- [32] R. Ma, B. Saxberg, C. Owens, N. Leung, Y. Lu, J. Simon, and D. I. Schuster, *Nature (London)* **566**, 51 (2019).
- [33] N. Yoshioka and R. Hamazaki, *Phys. Rev. B* **99**, 214306 (2019).
- [34] H. Weimer, *Phys. Rev. Lett.* **114**, 040402 (2015).
- [35] M. J. Hartmann and G. Carleo, *Phys. Rev. Lett.* **122**, 250502 (2019).
- [36] F. Vicentini, A. Biella, N. Regnault, and C. Ciuti, *Phys. Rev. Lett.* **122**, 250503 (2019).
- [37] F. Verstraete, J. J. García-Ripoll, and J. I. Cirac, *Phys. Rev. Lett.* **93**, 207204 (2004).
- [38] M. Zwolak and G. Vidal, *Phys. Rev. Lett.* **93**, 207205 (2004).
- [39] D. Kilda and J. Keeling, *Phys. Rev. Lett.* **122**, 043602 (2019).
- [40] A. Kshetrimayum, H. Weimer, and R. Orús, *Nat. Commun.* **8**, 1291 (2017).
- [41] H. Landa, M. Schiró, and G. Misguich, *Phys. Rev. Lett.* **124**, 043601 (2020).
- [42] J. Jin, A. Biella, O. Viyuela, L. Mazza, J. Keeling, R. Fazio, and D. Rossini, *Phys. Rev. X* **6**, 031011 (2016).
- [43] M. C. Gutzwiller, *Phys. Rev.* **137**, A1726 (1965).
- [44] W. F. Brinkman and T. M. Rice, *Phys. Rev. B* **2**, 4302 (1970).
- [45] D. S. Rokhsar and B. G. Kotliar, *Phys. Rev. B* **44**, 10328 (1991).
- [46] W. Krauth, M. Caffarel, and J.-P. Bouchaud, *Phys. Rev. B* **45**, 3137 (1992).
- [47] E. Kapit, M. Hafezi, and S. H. Simon, *Phys. Rev. X* **4**, 031039 (2014).
- [48] M. Scigliuzzo, G. Calajò, F. Ciccarello, D. Perez Lozano, A. Bengtsson, P. Scarlino, A. Wallraff, D. Chang, P. Delsing, and S. Gasparinetti, *Phys. Rev. X* **12**, 031036 (2022).
- [49] See Supplemental Material at <http://link.aps.org/supplemental/10.1103/PhysRevLett.131.193604> for additional details, which includes Refs. [50–58].
- [50] M.-D. Choi, *Linear Algebra Appl.* **10**, 285 (1975).
- [51] A. Jamiolkowski, *Rep. Math. Phys.* **3**, 275 (1972).
- [52] R. Balakrishnan, I. I. Satija, and C. W. Clark, *Phys. Rev. Lett.* **103**, 230403 (2009).
- [53] Y. Castin, in *Coherent Atomic Matter Waves*, edited by R. Kaiser, C. Westbrook, and F. David (EDP Sciences and Springer-Verlag, Berlin, 2001), pp. 1–136.
- [54] F. Baboux, D. D. Bernardis, V. Goblot, V. N. Gladilin, C. Gomez, E. Galopin, L. L. Gratiet, A. Lemaître, I. Sagnes, I. Carusotto, M. Wouters, A. Amo, and J. Bloch, *Optica* **5**, 1163 (2018).
- [55] E. Arrigoni and A. Dorda, in *Out-of-Equilibrium Physics of Correlated Electron Systems* (Springer International Publishing, Cham, 2018), pp. 121–188.
- [56] M. Seclì, Topology and nonlinearity in driven-dissipative photonic lattices: Semiclassical and quantum approaches, Ph.D. thesis, SISSA (International School for Advanced Studies), Trieste (2021).
- [57] G. C. and Z. P., *Quantum Noise* (Springer, Berlin, Heidelberg, 2004).
- [58] D. Walls and G. J. Milburn, *Quantum Optics* (Springer, Berlin, Heidelberg, 2008).
- [59] M. Biondi, G. Blatter, H. E. Türeci, and S. Schmidt, *Phys. Rev. A* **96**, 043809 (2017).
- [60] F. Caleffi, M. Capone, C. Menotti, I. Carusotto, and A. Recati, *Phys. Rev. Res.* **2**, 033276 (2020).
- [61] E. J. Mueller, T.-L. Ho, M. Ueda, and G. Baym, *Phys. Rev. A* **74**, 033612 (2006).
- [62] F. Minganti, A. Biella, N. Bartolo, and C. Ciuti, *Phys. Rev. A* **98**, 042118 (2018).
- [63] O. Scarlatella, R. Fazio, and M. Schiró, *Phys. Rev. B* **99**, 064511 (2019).
- [64] K. V. Krutitsky, *Phys. Rep.* **607**, 1 (2016).
- [65] M. Di Liberto, A. Recati, N. Trivedi, I. Carusotto, and C. Menotti, *Phys. Rev. Lett.* **120**, 073201 (2018).
- [66] Formally, the notion of particle-hole superfluidity is related to $R = \text{sgn}(\partial\rho_c/\partial n_0)$ at fixed J [64]. Nonetheless, we find that R does not change if calculated at fixed Ω for the same value of J [49].
- [67] K. V. Krutitsky and P. Navez, *Phys. Rev. A* **84**, 033602 (2011).
- [68] S. Stringari, *J. Exp. Theor. Phys.* **127**, 844 (2018).
- [69] L. M. Sieberer, M. Buchhold, and S. Diehl, *Rep. Prog. Phys.* **79**, 096001 (2016).

- [70] M. C. Cross and P. C. Hohenberg, *Rev. Mod. Phys.* **65**, 851 (1993).
- [71] L. P. Pitaevskii and S. Stringari, *Bose-Einstein Condensation and Superfluidity* (Oxford Science Publications, New York, 2016).
- [72] M. Wouters and I. Carusotto, *Phys. Rev. Lett.* **99**, 140402 (2007).
- [73] A. Chiocchetta and I. Carusotto, *Europhys. Lett.* **102**, 67007 (2013).
- [74] Y. Hidaka and Y. Minami, *Prog. Theor. Exp. Phys.* **2020**, 033A01 (2020).
- [75] A. Loirette-Pelous, I. Amelio, M. Seclì, and I. Carusotto, *Phys. Rev. A* **104**, 053516 (2021).
- [76] M. Wouters and I. Carusotto, *Phys. Rev. B* **79**, 125311 (2009).
- [77] C. Ciuti and I. Carusotto, *Phys. Rev. A* **74**, 033811 (2006).
- [78] A. Chiocchetta, A. Gambassi, and I. Carusotto, Laser operation and Bose-Einstein condensation: Analogies and differences, in *Universal Themes of Bose-Einstein Condensation* (Cambridge University Press, Cambridge, England, 2017), pp. 409–423.
- [79] O. Scarlatella, A. A. Clerk, and M. Schiró, *New J. Phys.* **21**, 043040 (2019).
- [80] O. Scarlatella, A. A. Clerk, R. Fazio, and M. Schiró, *Phys. Rev. X* **11**, 031018 (2021).
- [81] E. Boukobza and D. J. Tannor, *Phys. Rev. A* **74**, 063822 (2006).
- [82] E. Boukobza and D. J. Tannor, *Phys. Rev. Lett.* **98**, 240601 (2007).
- [83] O. Scarlatella, A. A. Clerk, and M. Schiró, *arXiv:2303.09673*.
- [84] M. Wouters and I. Carusotto, *Phys. Rev. B* **79**, 125311 (2009).